Monolayer of amphiphilic functionalized gold nanoparticles at an air-water interface

Raj Kumar Gupta,[1,2,*] K. A. Suresh,[2] and Sandeep Kumar[2]
[1]*Birla Institute of Technology and Science, Pilani, Physics Group, Rajasthan 333031, India*
[2]*Raman Research Institute, Sadashivanagar, Bangalore 560080, India*
(Received 1 July 2008; published 18 September 2008)

Langmuir films at the air-water interface exhibit a variety of surface phases which arise primarily due to the molecular interaction governed by intermolecular separation. We have studied the thermodynamical aspects of Langmuir monolayers of amphiphilic functionalized gold nanoparticles (AGNs) at the air-water (*A*-*W*) interface. Interestingly, the AGN monolayer exhibits phases like gas, a low-ordered liquid (L_1), a high-ordered liquid (L_2), and a collapsed state. We find that the first-order phase transition between L_1 and L_2 vanishes above a critical temperature of 28.4 °C. Surprisingly, for a range of higher temperatures ($\geqslant$29.4 °C and $\leqslant$36.3 °C), the L_1 phase undergoes a transition to a bilayer of the L_2 phase before entering into the collapsed state.

DOI: 10.1103/PhysRevE.78.032601 PACS number(s): 68.47.Pe, 68.37.−d

In the last 20 years, the field of nanoscience and nanotechnology has made enormous growth because of its potential industrial applications [1]. The properties of the materials change drastically when its dimensions scale down to nanometer length scale [2]. Nanoparticles can be forced to assemble on superlattices whose optical and electronic properties are tunable. One of the important parameters determining the properties of nanoparticle crystals is the interparticle separation. Other parameters are the charging energy of the particles, the strength of the interaction between the particles, and the symmetry of the lattice formed by the particles [3,4]. The interparticle separation can precisely be maneuvered by forming the monolayer of the nanoparticles at an interface and changing the surface density. A stable monolayer at the air-water (*A*-*W*) interface is known as a Langmuir monolayer. The Langmuir monolayer is an ideal system for studying the thermodynamics of two-dimensional (2D) systems and the nature of interactions involved between the particles [5]. Changing the interparticle distances by the lateral compression of the monolayer, different 2D phases can be obtained [6]. These phases can be transferred layer by layer onto different substrates by the Langmuir-Blodgett (LB) technique [5]. Interestingly, Collier and co-workers have reported a metal-insulator transition in the Langmuir monolayer of hydrophobic silver nanoparticles at the *A*-*W* interface [7,8]. They observed a quantum interference between the particles which was governed by interparticle distances. A few other attempts have been made to study the Langmuir monolayer of the functionalized metal nanoparticles at the *A*-*W* interface [9–13]. However, the particles studied so far did not show a stable Langmuir monolayer. The important criterion for the formation of stable Langmuir monolayers at the *A*-*W* interface is that the particles should be amphiphilic in nature with a proper balance between their hydrophilic and hydrophobic parts [5]. Accordingly, we synthesized amphiphilic gold nanoparticles (AGNs) functionalized with hydroxy-terminated alkyl-thiol and studied the Langmuir film of the particles by surface manometry and microscopy techniques. We find a stable Langmuir monolayer of the AGNs at the *A*-*W* interface. The monolayer exhibits gas, low-ordered liquid (L_1), high-ordered liquid (L_2), bilayer of L_2 (Bi), and the collapsed states. The first-order phase transition between L_1 and L_2 is accompanied by a coexistence of the two phases. The coexisting region of L_1 and L_2 vanishes above a critical temperature of 28.4 °C. Based on our studies, we construct a phase diagram showing the phases observed during the compression of the monolayer at the *A*-*W* interface at different temperatures.

The amphiphilic AGNs were synthesized in the laboratory [14]. It has been well established that this synthesis procedure ensures uniformly coated nanoparticles. The size of the particles was estimated from transmission electron microscope (TEM) images (Fig. 1). The particles had a mean core diameter of 5.5 nm with a standard deviation of ±1 nm. The diameter of the AGNs for the fully stretched ligands was calculated as 8.4 nm. Hence, the mean cross-sectional area of each particle thus calculated was 55.4 nm^2.

A solution of 0.1 mg/ml of AGNs was prepared in 80% toluene and 20% methanol. The monolayer was formed by spreading the solution on ultrapure ion-free water (MilliQ, Millipore) in a LB trough (NIMA 611M). The monolayer was compressed symmetrically by the coupled barriers of the

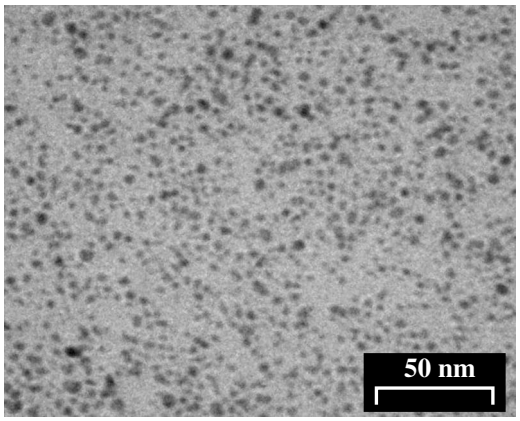

FIG. 1. Transmission electron microscope (Hitachi, H7000, 100 kV) image of the AGN. The solution of the sample of AGN was spread on a carbon-evaporated copper grid, and the image was scanned after 2 h.

*raj@bits-pilani.ac.in

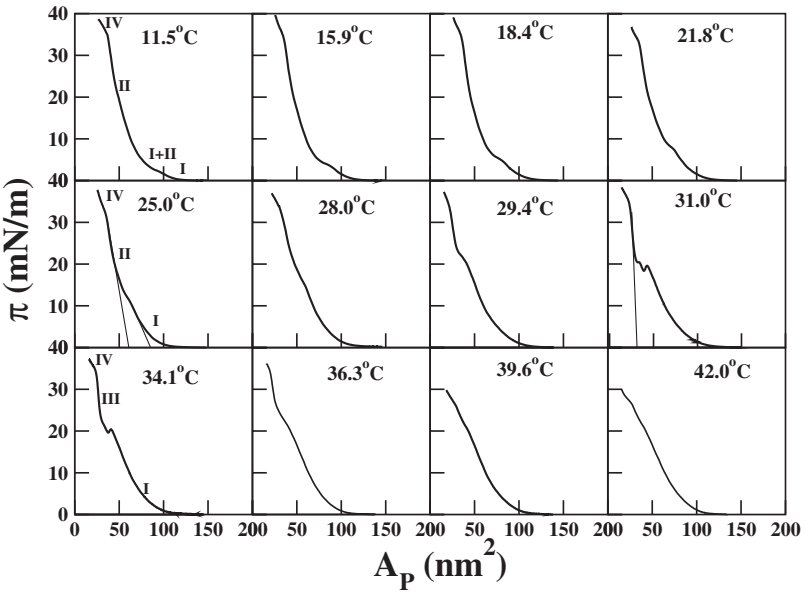

FIG. 2. Surface pressure (π)-area per particle (A_P) isotherms of AGNs at different temperatures. The symbols I, II, III, and IV denote L_1, L_2, Bi, and collapsed regions in the isotherms, respectively. The straight lines in the isotherms for temperatures 25 and 31 °C are shown as the extrapolated lines for calculating the average area occupied by each particle in the respective phases. The error incurred in such a calculation is ± 1%.

trough at a compression speed of 10.7 (nm^2/particle)/min. The temperature (T) of the subphase was maintained by the water circulation method using a temperature controller (Julabo, F25-MV, thermal stability= ± 0.01 °C). The Brewster angle microscope (BAM) experiments were done using MiniBAM Plus (Nanofilm Technologie). The monolayers of the AGNs at different phases were transferred onto solid substrates by the LB technique. The substrates were prepared by thermally evaporating gold on glass plates [15]. The transfer ratios of the LB films were 1 ± 0.1. The reflection absorption infrared spectroscopy (RAIRS) was done using a homebuilt grazing angle setup (angle of reflection=86°) and a Fourier-transform infrared (FTIR) spectrometer (Shimadzu, FT8400) having a spectral resolution of 4 cm^{-1}. The spectra of the transfered monolayer were recorded immediately after the LB deposition.

The surface pressure (π)-area per particle (A_P) isotherms of AGNs at different temperatures (Fig. 2) show zero surface pressure at very large A_P, indicating a coexistence of gas and a low-density liquid (L_1) phase. On reducing A_P (monolayer compression), the gas phase disappears and the isotherms show lift-off area per particle to be around 120 nm^2. On compressing the monolayer, the isotherms show a slow and gradual rise in surface pressure. This is the pure L_1 phase. The extrapolation of the region of the isotherm to the zero surface pressure on the A_P axis yields the average area occupied by the particles in that particular phase [5]. The average particle area in the L_1 phase at 25 °C was 85 nm^2. On compressing the monolayer below 28 °C, the slow and gradual rise in surface pressure is accompanied by a plateau in the isotherms. On further compression, the surface pressure rises sharply until the monolayer collapses at A_P ~ 36 nm^2. The region of the isotherm with the sharp rise in surface pressure can correspond to a high-density liquid (L_2) phase. At 25 °C, the average particle area in the L_2 phase was around 61 nm^2. This value nearly corresponds to the mean cross-sectional area of the particles determined through TEM images. The small difference in the value may be due to the polydispersity in the size distribution of the particles. The appearance of plateaus in the isotherms suggests a first-order phase transition between L_1 and L_2 phases. The coexistence of two phases is denoted as I+II in the isotherms. The phase-coexisting plateau region decreases with increasing T and finally vanishes above a critical temperature (T_c). The T_c was calculated by plotting the enthalpy of the L_1-L_2 transition with respect to T and extrapolating it to a zero value on the T axis [16]. We obtain a T_c value of 28.4 °C for this transition. These behaviors have been observed and understood in the case of standard amphiphilic molecules like phospholipids [17–19]. The isotherms indicate a smooth collapse of the monolayer. This may be due to the isotropic shape of the particles. Such smooth collapses were also observed in the case of spherical core functionalized fullerene derivatives [20,21]. The reversibility of the isotherms was studied by successive compression and expansion of the monolayer at 25 °C. We find the monolayer to be highly reversible. The stability of the phases was also tested qualitatively by holding the surface pressure at a given value and monitoring the drop in A_P. We find almost no variation in A_P over a long period of time. These observations suggest the monolayer of AGNs at the A-W interface to be very stable.

The π-A_P isotherms obtained in the range 28.4 °C $\leqslant T \leqslant$ 36.3 °C show interesting behaviors. The isotherms show the usual L_1 phase. On reducing the A_P, the L_1 phase appears to collapse by introducing an unstable region in the isotherm. However, on further reducing A_P, the isotherms indicate a steep rise in surface pressure and then a smooth-collapse-like feature. Extrapolating the steep region to the zero surface pressure yields a value of ~31 nm^2 at 31 °C. This value is nearly twice that obtained for the L_2 phase (61 nm^2). Hence, this phase can presumed to be a bilayer (Bi) of the L_2 phase. The unstable region of isotherms leading to the transition from the L_1 to the Bi phase can be considered as a coexistence region. The coexistence region initially increases up to 31 °C, but decreases thereafter until it vanishes above 36.3 °C. The Bi phase also disappears above 36.3 °C. Thereafter, the monolayer showed gas, L_1, and the collapsed states.

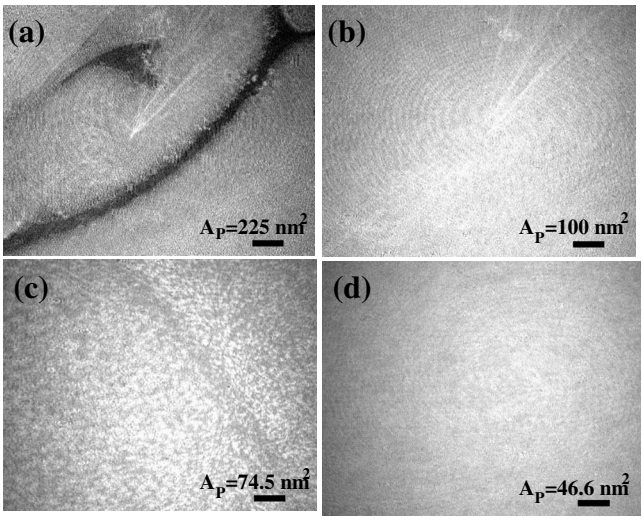

FIG. 3. The BAM images of the monolayer of AGN at 18.4 °C taken at different A_P. (a) A coexistence of dark and gray regions, (b) a uniform gray region, (c) a coexistence of bright domains on the gray background, and (d) a uniform bright region. Scale bar =500 μm.

In Brewster angle microscopy, the intensity levels in images depend on the surface density and thickness of the films [22].

The BAM image [Fig. 3(a)] at a large A_P shows a coexistence of dark and gray regions. The dark region vanishes on compression, leading to a uniform gray texture [Fig. 3(b)]. The gray domains appeared fluidic and mobile under the microscope. The dark region represents the gas phase, whereas the gray domains correspond to the low-density liquid (L_1) phase. The image [Fig. 3(c)] corresponding to the plateau region of the isotherms shows bright domains in the gray background. On compression, the bright domains grow at the expense of the gray region, leading to a uniform bright texture [Fig. 3(d)]. The uniform bright texture, obtained in region II of the isotherm, corresponds to the high-density liquid (L_2) phase. The coexistence of L_1 and L_2 domains in the plateau region of the isotherm establishes a first-order phase transition between the phases. The BAM images in the collapsed state showed a wrinkled structure. The wrinkled structure might appear due to folding of the AGN monolayer [23,24].

The BAM images of the monolayer of AGNs at 31 °C showed the gas (dark region) and L_1 phases (gray region) at large A_P. The gas phase disappears on compressing the monolayer, leading to a uniform L_1 phase. The L_1 phase continues to exist until monolayer destabilizes at $A_P \sim 44$ nm^2. Such destabilization leads to the nucleation and growth (Fig. 4) of the very bright domains on the gray background. The bright domains grow at the expense of the gray region, finally leading to a uniform bright region. The bright region was obtained in the region of the isotherm corresponding to a steep rise in the surface pressure after the destabilization. The bright region corresponds to the bilayer of the L_2 (Bi) phase. The bright region (Bi phase) also collapses on compression, leading to a wrinkled structure.

In RAIRS, the absorbance due to film deposited in a

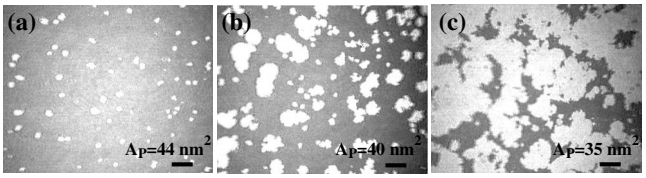

FIG. 4. The BAM images of the monolayer of AGNs at 31 °C taken at different A_P. (a)–(c) Nucleation and growth of bright domains on the gray background. Scale bar=500 μm.

phase α (Γ_α) is proportional to the thickness (d_α) and the surface concentration (C_α) of the film. Hence, for the two different phases α and α', it can be written as

$$\frac{\Gamma_\alpha}{\Gamma_{\alpha'}} = \left(\frac{C_\alpha}{C_{\alpha'}}\right)\left(\frac{d_\alpha}{d_{\alpha'}}\right). \quad (1)$$

RAIRS on the LB films of AGNs was performed for the determination of the relative surface concentration ($C_\alpha/C_{\alpha'}$) and relative thickness ($d_\alpha/d_{\alpha'}$) of the films in different phases (Fig. 5). We have analyzed the peaks corresponding to the asymmetric stretching of the $-CH_2$ and $-CH_3$ groups of the alkyl chain of the funtionalized gold nanoparticles. The asymmetric stretches for both groups were not well split. Nonetheless, they together contribute to a well-defined peak from 2890 to 2988 cm^{-1} (Fig. 5).

The area under a peak yields integrated absorbance. The integrated absorbance (Γ), for the L_1 (Γ_{L_1}), L_2 (Γ_{L_2}), and the Bi (Γ_{Bi}) phases was found to be 65, 83, and 164 (arbitrary units), respectively. Assuming $d_{L_1} \approx d_{L_2}$, the observed difference in Γ's can be attributed to the difference in C's of the LB films of AGNs in the two phases. Employing Eq. (1), the relative concentration of L_2 phase with respect to L_1 phase (C_{L_2}/C_{L_1}) was found to be 1.28. From π-A_P isotherms, the C_α of AGN particles in a particular phase (α) can be determined by taking the inverse of the extrapolated area per particle. The isotherm at 25 °C yields C_{L_1} and C_{L_2} to be 0.012 and 0.016 particles per nm^2, respectively (Fig. 2). Hence, the

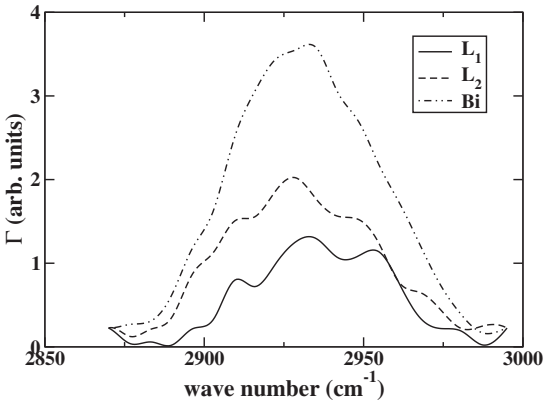

FIG. 5. The RAIRS spectra for the LB films of AGNs on a gold substrate deposited in different phases as shown in the inset. The L_1 and L_2 phases were transferred at 24 °C and at the surface pressures of 4 and 20 mN/m, respectively. The Bi phase was transfered at 31.5 °C and at a surface pressure of 27 mN/m.

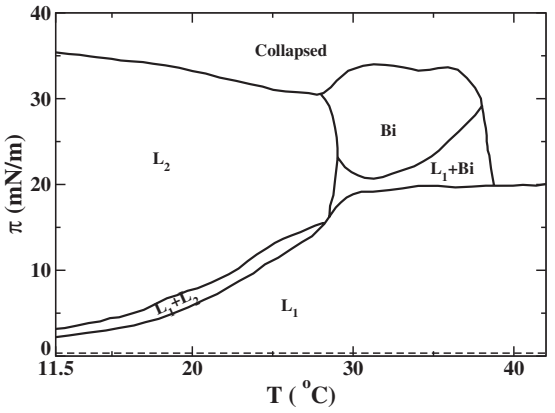

FIG. 6. The phase diagram showing the observed 2D phases of the Langmuir monolayer of AGNs at the A-W interface. The L_1- and gas-phase coexistence was seen even at very large A_P and zero π. This is shown by the dotted line. The L_1, L_2, and Bi are the low-ordered layer, high-ordered layer, and bilayer of L_2 phases, respectively. The coexistence of the phases are shown by the "+" symbol.

ratio C_{L_2}/C_{L_1} obtained from the isotherm was found to be 1.3. This value is nearly same as compared to the one obtained from the RAIRS experiment. Similarly, in the case of LB film of Bi phase, assuming $C_{L_2} \approx C_{\mathrm{Bi}}$, the change in Γ's is due to the change in thickness of the films. Using Eq. (1), the ratio d_{Bi}/d_{L_2} was found to be ~ 2, confirming the Bi phase to be a bilayer of the L_2 phase.

Based on our studies, we construct (Fig. 6) a phase diagram of the Langmuir monolayer of AGNs at the A-W interface.

The AGNs can be approximated to isotropic in shape; hence, the phase transitions in the Langmuir monolayer of the particles are essentially due to the change in interparticle distances and the ordering among them. For the range of $11.5\ ^\circ\mathrm{C} \leqslant T \leqslant 28.0\ ^\circ\mathrm{C}$, the transition surface pressure between L_1 and L_2 increases with the increase in T. The positive slope $(d\pi/dT)$ of the L_1-L_2 transition curve indicates a decrease in the entropy during the transition [16]. This observation suggests a higher degree of orderness of the L_2 phase as compared to that of the L_1 phase. The maximum in-plane elastic modulus of the two phases (i.e., L_1 and L_2) at $18.4\ ^\circ\mathrm{C}$ were merely 17.6 and 48.4 mN/m (error $\sim \pm 0.5\%$), respectively. These are low as compared to the liquid-expanded and liquid-condensed phases of phospholipids [17]. Based on the π-T slope, elastic modulus, and BAM images, we define the L_1 as a low-ordered liquid phase and L_2 as a high-ordered liquid phase. Interestingly, the T range from 29.4 to $36.3\ ^\circ\mathrm{C}$ and a surface pressure range from around 17 to 35 mN/m showed the Bi phase. Above $36.3\ ^\circ\mathrm{C}$, the monolayer exhibits gas, L_1, and collapsed states.

We observed a stable Langmuir monolayer of AGNs at the A-W interface. The monolayer exhibits a variety of phases like gas, low-order liquid (L_1), high-ordered liquid (L_2), bilayer of L_2 (Bi), and collapsed states. We believe that this is the first report on such a system exhibiting interesting surface phases. The electronic and optical properties of the phases on the different solid substrates will be probed in order to acquire a better understanding of the structural dependence of the films on such properties.

[1] M.-C. Daniel and D. Astruc, Chem. Rev. (Washington, D.C.) **104**, 293 (2004).
[2] G. Hodes, Adv. Mater. (Weinheim, Ger.) **19**, 639 (2007).
[3] Y. Min *et al.*, Nat. Mater. **7**, 527 (2008).
[4] P. Zhang and T. K. Sham, Phys. Rev. Lett. **90**, 245502 (2003).
[5] G. L. Gaines, Jr., *Insoluble Monolayers at Liquid-gas Interfaces* (Interscience, New York, 1966).
[6] V. M. Kaganer, H. Möhwald, and P. Dutta, Rev. Mod. Phys. **71**, 779 (1999).
[7] C. P. Collier *et al.*, Science **277**, 1978 (1997).
[8] G. Markovich, C. P. Collier, and J. R. Heath, Phys. Rev. Lett. **80**, 3807 (1998).
[9] J. R. Heath, C. M. Knobler, and D. V. Leff, J. Phys. Chem. B **101**, 189 (1997).
[10] A. Swami *et al.*, J. Colloid Interface Sci. **260**, 367 (2003).
[11] I. A. Greene *et al.*, J. Phys. Chem. B **107**, 5733 (2003).
[12] J. J. Brown *et al.*, Langmuir **17**, 7966 (2001).
[13] M. Fukuto *et al.*, J. Chem. Phys. **120**, 3446 (2004).
[14] Y. Song, T. Huang, and R. W. Murray, J. Am. Chem. Soc. **125**, 11694 (2003).
[15] R. K. Gupta and K. A. Suresh, Eur. Phys. J. E **14**, 35 (2004).
[16] H. B. Callen, *Thermodynamics and an Introduction to Thermostatistics*, 2nd ed. (Wiley, New York, 1985).
[17] H. Möhwald, in *Phospholipid Monolayers*, edited by R. Lipowsky and E. Sackmann, *Handbook of Biological Physics*, Vol. 1 (Elsevier, Amsterdam, 1995), Chap. 4.
[18] K. S. Birdi, *Lipid and Biopolymer Monolayers at Liquid Interfaces* (Plenum, New York, 1989).
[19] S. Baoukina *et al.*, Langmuir **23**, 12617 (2007).
[20] L. Leo *et al.*, Langmuir **16**, 4599 (2000).
[21] J. -L. Gallani *et al.*, Langmuir **18**, 2908 (2002).
[22] S. Rivière *et al.*, J. Chem. Phys. **101**, 10045 (1994).
[23] W. Lu, C. M. Knobler, R. F. Bruinsma, M. Dennin, and M. Twardos, Phys. Rev. Lett. **89**, 146107 (2002).
[24] A. Gopal and K. Y. C. Lee, J. Phys. Chem. B **105**, 10348 (2001).